



1 Motivation [1, 2]

Whenever at a plasma boundary the plasma potential falls inside an energy gap, polarisation-induced external surface states (image states) exist. Provided a plasma electron approaching the boundary can get rid of its excess energy it may get trapped (adsorbed) in these surface states. Once trapped it may de-trap again (desorb) if it gains enough energy from the surface. Hence in addition to elastic and inelastic scattering, the interaction of plasma electrons with boundaries encompasses physisorption, the polarisation-induced temporary binding of an electron to the surface which may be characterised by the electronic sticking coefficient s_e and the electronic desorption time τ_e . Physisorption in the surface states may lead to a quasi-stationary film of electrons at the surface. We propose that this process leads to the build-up of surface charges at plasma boundaries.

In the following, we are interested in physisorption of image-bound electrons at dielectric surfaces, appearing as plasma boundaries in dusty plasmas (e.g. graphite) and dielectric barrier discharges. Relaxation channels arising from the creation and annihilation of internal electron-hole pairs being closed because of the large energy gap, electron energy relaxation, leading to sticking and desorption, is provided by the creation and annihilation of phonons.

2 Theory [2]

2.1 Electron kinetics

The time evolution of the occupancies of the bound surface states during a desorption process is given by

$$\frac{d}{dt}n_q(t) = \sum_{q'} [W_{qq'}n_{q'}(t) - W_{q'q}n_q(t)] - W_{cq}n_q(t), \quad (1)$$

where $W_{qq'}$ and W_{cq} are the probabilities for a transition from bound state q' to bound state q and for a transition from bound state q to the continuum, respectively.

To solve equation (1) the eigenvalue equation for the matrix comprising the transition probabilities has to be solved. If the transitions to the continuum are much slower than the transitions between bound states, one eigenvalue, λ_0 , is considerably smaller than all the other eigenvalues λ_κ . Then, the general solution of equation (1) is

$$n_i(t) = f^{(0)}e_i^{(0)}e^{-\lambda_0 t} + \sum_{\kappa>0} f^{(\kappa)}e_i^{(\kappa)}e^{-\lambda_\kappa t}, \quad (2)$$

where λ_0 governs the long time behaviour of the equilibrium occupation of the bound states, $e_i^{(0)} = n_i^{\text{eq}} \sim e^{-E_i/k_B T_s}$. Hence, we identify this eigenvalue with the inverse of the desorption time,

$$\tau_e^{-1} = \lambda_0. \quad (3)$$

The likelihood for an incident electron in the continuum state k to get stuck to the surface is given by the prompt energy resolved sticking coefficient

$$s_{e,k}^{\text{prompt}} = \sum_q \tau_t W_{qk}, \quad (4)$$

where τ_t is the travelling time through the surface potential well of width L which drops out once $L \rightarrow \infty$ and W_{qk} is the transition probability from the continuum state k to the bound state q . Provided that the energy of the incident electrons is Boltzmann distributed for the temperature $T_e = 1/k_B \beta_e$, the energy averaged sticking coefficient - the global sticking coefficient - is given by

$$s_e = \frac{\sum_k s_{e,k} k e^{-\beta_e E_k}}{\sum_k k e^{-\beta_e E_k}}. \quad (5)$$

Sticking occurs in several stages. First the electron makes a transition from the continuum to a bound state, then a cascade of fast transitions between bound states leads to the stationary equilibrium distribution, and finally the electron desorbs. The kinetic sticking coefficient gives the probability of making a transition to a bound state and subsequent relaxation. It can be computed from the prompt sticking coefficient and the time evolution of the bound state occupancy during desorption. The kinetic energy resolved sticking coefficient reads

$$s_{e,k}^{\text{kinetic}} = \tau_t \sum_{q,q'} \tilde{e}_q^{(0)} e_q^{(0)} W_{q,k}, \quad (6)$$

where $e^{(0)}$ and $\tilde{e}^{(0)}$ are the right and left eigenvector to λ_0 .

2.2 Electron-surface interaction

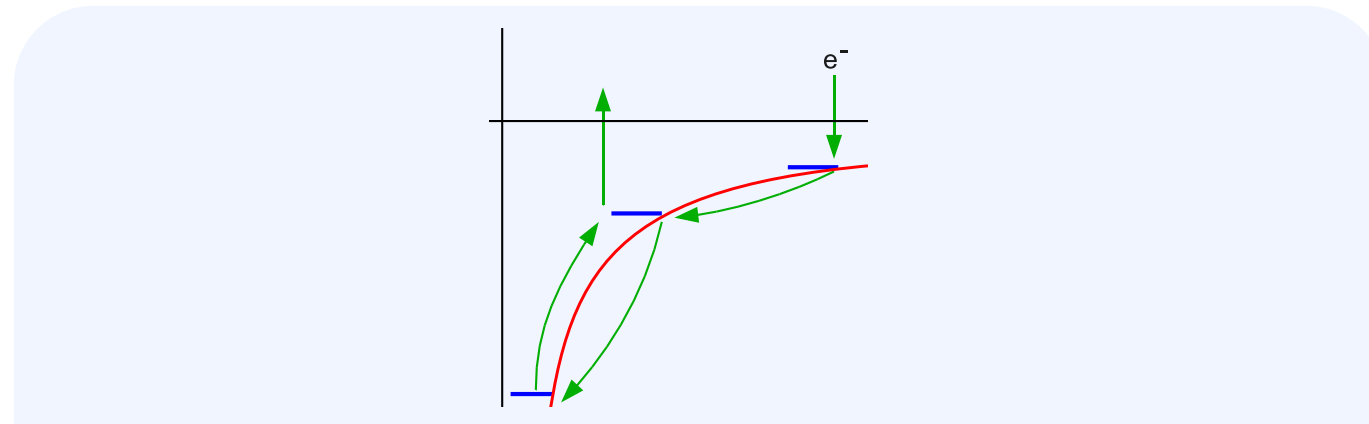


Fig. 1: Microphysics of an electron at a dielectric surface: surface potential (red), surface states (blue). Surface vibrations trigger transitions of the electron (exemplified by green arrows).

Fig. 1 gives an overview over the relevant microscopic processes: A coupling of the electron to dipole-active optical surface phonons leads to the static surface potential which exhibits surface states. Far from the surface this potential is the classical image potential but close to the surface it is strongly modified by the recoil energy resulting from the momentum transfer parallel to the surface when the electron absorbs or emits a surface phonon. Surface vibrations arising from the longitudinal acoustic phonon perpendicular to the surface induce transitions between the surface states.

Hence, the Hamiltonian for the surface electron can be split into three parts,

$$H = H_e^{\text{static}} + H_{ph} + H_{e-ph}^{\text{dyn}}, \quad (7)$$

where the H_e^{static} represents the electron in the static surface potential, H_{ph} the free acoustic phonons and H_{e-ph}^{dyn} the dynamic perturbation due to surface vibrations, which can be expanded with respect to the displacement field u , giving rise to one-phonon, two-phonon and three-phonon transitions etc. .

2.3 Potential depth classification

The depth of the surface potential can be classified with respect to the maximum energy of the acoustic phonon - in our model the Debye energy. We call the surface potential

- shallow if the lowest bound state is at most one Debye energy beneath the continuum,
- one-phonon deep if the energy difference between the lowest two bound states is less than one Debye energy,
- two-phonon deep if the energy difference between the lowest two bound states is between one and two Debye energies.

Since physisorption of electrons typically takes place in at least two-phonon deep surface potentials, sticking and desorption of electrons has to be controlled by multi-phonon processes (see Table 1).

	ϵ	$k_B T_D$	ΔE_{12}	$\Delta E_{12}/k_B T_D$
graphite	13.5	0.215 eV	0.233 eV	1.06
GaAs	13	0.030 eV	0.152 eV	5.13

Table 1: Dielectric constant ϵ , Debye energy $k_B T_D$, energy difference of the lowest two bound states of the recoil-corrected image potential ΔE_{12} , and potential depth for different dielectrics.

2.4 Transition rates

The transition rate from an electronic state q to an electronic state q' is given by

$$\mathcal{R}(q', q) = \frac{2\pi}{\hbar} \sum_{s,s'} \frac{e^{-\beta E_s}}{\sum_{s''} e^{-\beta E_{s''}}} |\langle s', q' | T | s, q \rangle|^2 \times \delta(E_s - E_{s'} + E_q - E_{q'}), \quad (8)$$

where T is the T -matrix corresponding to H_{e-ph}^{dyn} and $\beta = (k_B T_s)^{-1}$ with T_s the surface temperature; $|s\rangle$ and $|s'\rangle$ are initial and final phonon states, which are averaged over.

In general, multi-phonon processes have two possible origins: (i) multi-phonon terms in H_{e-ph}^{dyn} and (ii) multiple actions of the perturbation as encoded in the T -matrix.

The one-phonon process is accounted for by

$$\langle s', q' | V_1 | s, q \rangle \langle s, q | V_1^* | s', q' \rangle, \quad (9)$$

the standard golden rule approximation, where V_1 is the term in T of $\mathcal{O}(u)$.

Most two-phonon terms are merely corrections to the one-phonon process. Thus for transitions already

triggered by a one-phonon process we neglect, in a first approximation, these correction terms. Then,

$$\begin{aligned} & \langle s', q' | V_2 | s, q \rangle \langle s, q | V_2^* | s', q' \rangle, \\ & \langle s', q' | V_2 | s, q \rangle \langle s, q | V_1^* G_0^* V_1^* | s', q' \rangle, \\ & \langle s', q' | V_1 G_0 V_1 | s, q \rangle \langle s, q | V_2^* | s', q' \rangle, \\ & \langle s', q' | V_1 G_0 V_1 | s, q \rangle \langle s, q | V_1^* G_0^* V_1^* | s', q' \rangle, \end{aligned} \quad (10)$$

where V_2 and $V_1 G_0 V_1$ are the terms in T of $\mathcal{O}(u^2)$, inducing transitions not already triggered by the one-phonon process.

3 Results [2]

Except for the Debye temperature T_D , the material parameters used for the numerical calculation apply to graphite (for graphite $T_D = 2500K$).

3.1 Desorption

Figure 2 shows that the inverse desorption time, τ_e^{-1} , depends strongly on the surface temperature, varying several orders of magnitude when the surface temperature changes.

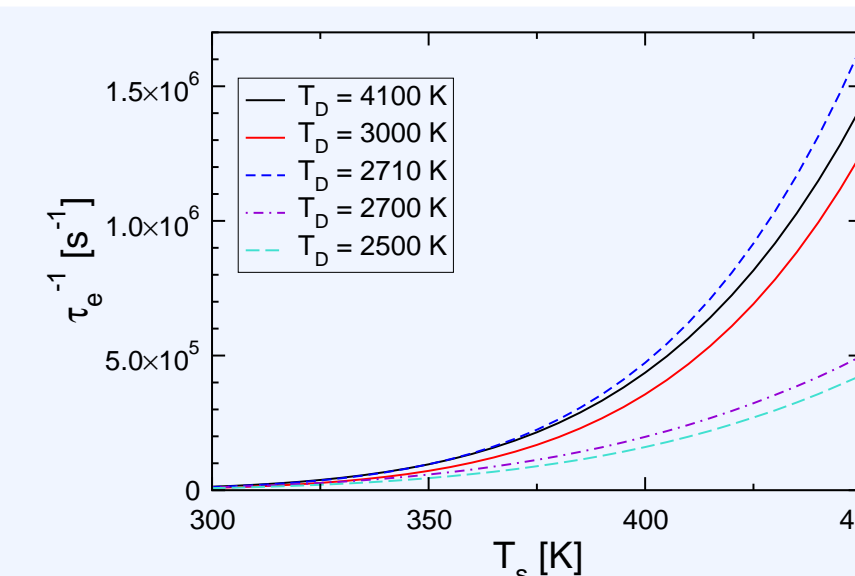


Fig. 2: Inverse desorption time τ_e^{-1} as a function of the surface temperature. For high surface temperatures desorption from a two phonon deep potential ($T_D = 2700K, 2500K$) is significantly slower than desorption from a one-phonon deep potential ($T_D = 2710K, 3000K$) or a shallow potential ($T_D = 4100K$).

For a surface temperature of $360K$, we find for graphite ($T_D = 2500K$) an electron desorption time $2 \cdot 10^{-5}s$. We also investigated, as a function of the potential depth, the relative importance of direct vs. cascading desorption channels. For that purpose we use the Debye energy as an adjustable parameter (see Fig. 3).

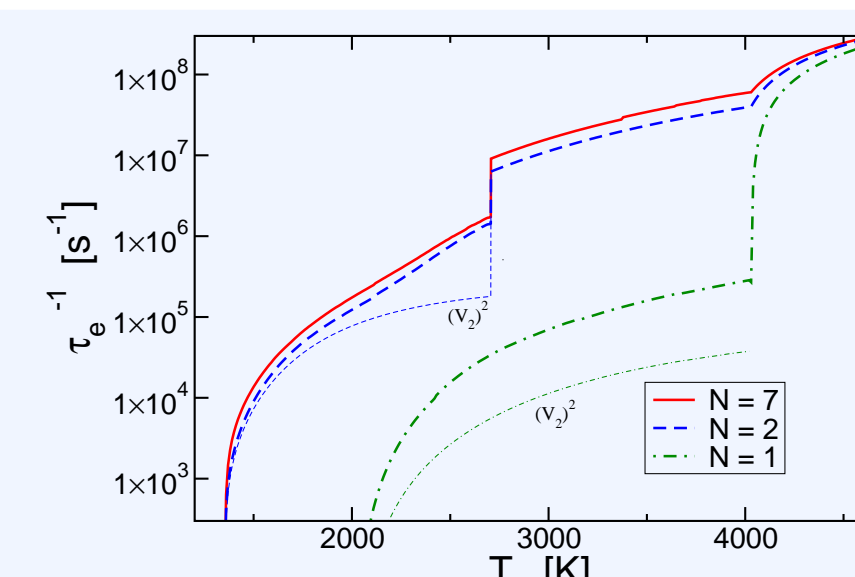


Fig. 3: Inverse desorption time τ_e^{-1} for $\delta = T_D/T_s = 5$ as a function of the Debye temperature T_D calculated with different numbers of bound states N . Above $T_D = 2010K$ the continuum is accessible from the lowest bound state by two-phonon processes, above $T_D = 4029K$ by one-phonon processes. For $T_D < 2707K$ the potential is two-phonon deep, for $2707K < T_D < 4029K$ it is one-phonon deep and above $T_D = 4029K$ it is shallow. For the thin lines the two-phonon process has been calculated using the two-phonon process $(V_2)^2$ (cf. (10)) only.

Depending on the depth of the surface potential we identify various desorption scenarios (see Fig. 4). For a shallow potential, the lowest bound state can be emptied most efficiently by direct one-phonon transitions to the continuum. For a one-phonon deep potential the direct two-phonon process to the continuum is superseded by a cascade via the second bound state as the most efficient desorption channel. Even for a two-phonon deep potential the cascade via the second level dominates, albeit with a two-phonon process between the lowest and second lowest bound state.

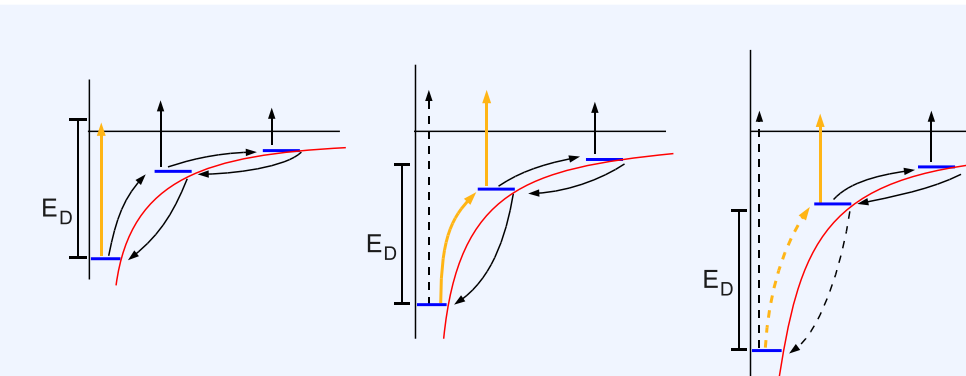


Fig. 4: Desorption channels depending on the potential depth for a shallow (left panel), one-phonon deep (middle panel) and two-phonon deep potential (right panel). Predominant channel bold orange, one-phonon processes full lines, two-phonon processes dashed lines.

3.2 Sticking

Steep jumps in the energy resolved sticking coefficient (see Fig. 5) reflect bound state accessibility. One-phonon processes, if applicable, provide

for much larger sticking coefficients than two-phonon processes.

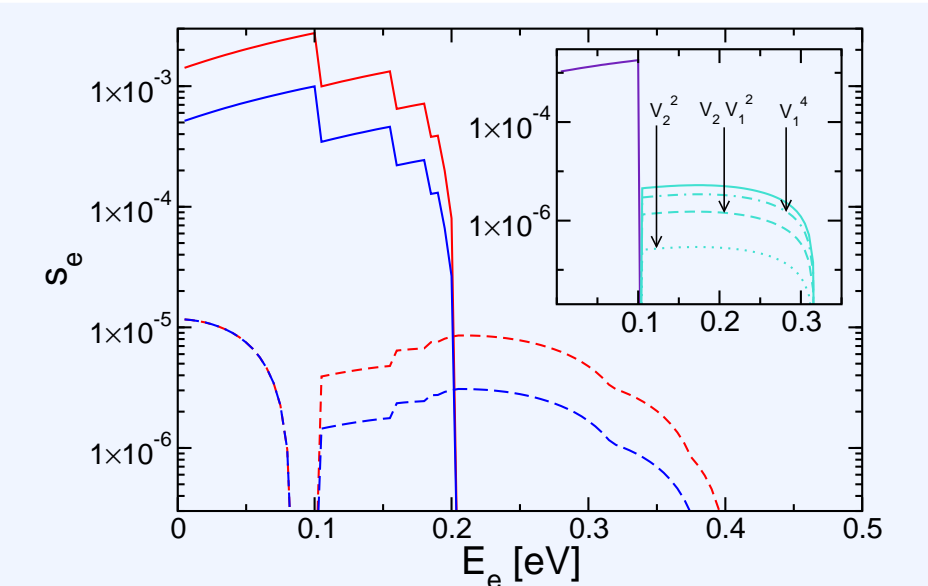


Fig. 5: Prompt (red) and kinetic (blue) energy resolved sticking coefficient for a two-phonon deep potential ($T_D = 2500K$) at $T_s = 357K$. Full line one-phonon contribution, dashed line two-phonon contribution. Inset: Contribution of the second bound state. One-phonon contribution (violet), two-phonon contribution (turquoise) broken down into the processes $(V_2)^2$, $(V_1)^2 V_2$ and $(V_1)^4$ (cf. (10)).

For one-phonon deep potentials the relaxation of a trapped electron is controlled by fast one-phonon cascades so that kinetic and prompt sticking coefficient differ very little. For two-phonon deep potentials the two-phonon process required for reaching the lowest level leads to a temperature dependent relaxation bottleneck, resulting in a pile-up of trapped electrons in the upper bound state and hence a large reduction of the kinetic vs. the prompt sticking coefficient (see Fig. 6).

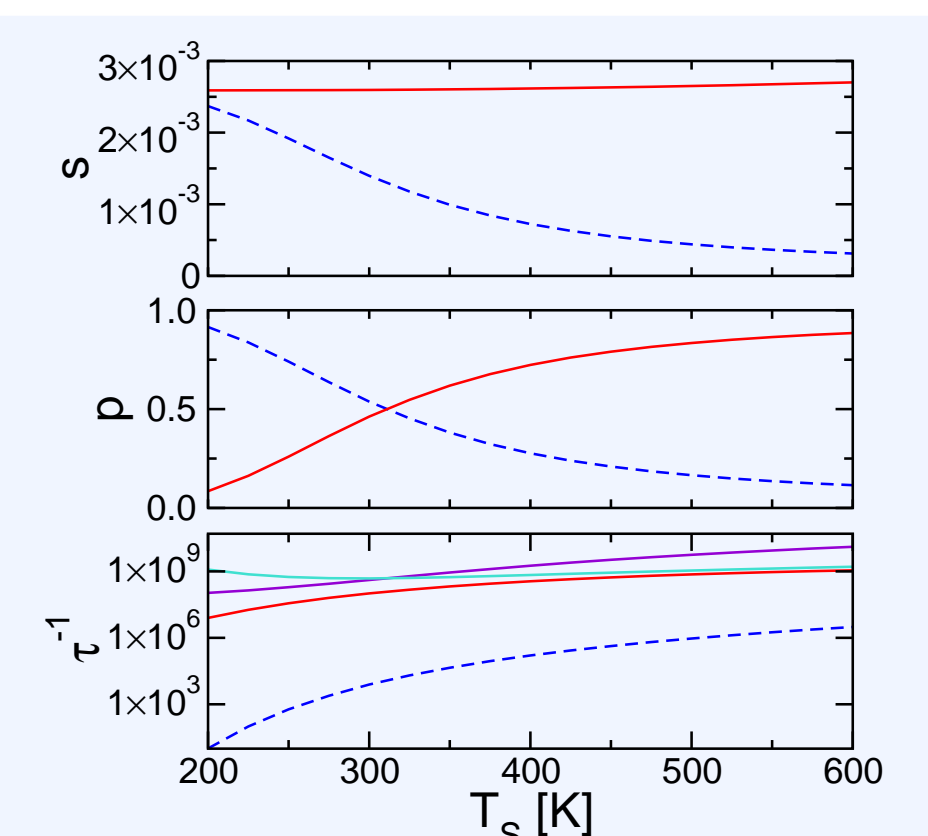


Fig. 6: Upper panel: Prompt (full red line) and kinetic (dashed blue line) energy resolved sticking coefficient for an electron energy of $E_e = 0.09eV$ in a two-phonon deep potential ($T_D = 2500K$) as a function of the surface temperature. Middle panel: Probability for an electron initially trapped in one of the upper bound states to either fall to the lowest bound state (dashed blue line) or to desorb without ever reaching the lowest bound state (full red line). Lower panel: Inverse desorption time (dashed blue line), inverse desorption time for a surface potential lacking the lowest bound state (full red line) and conditional mean first-passage times for an electron trapped in the upper bound states to the lowest bound state (turquoise) or to the continuum (violet).

The strong temperature dependence of the kinetic sticking coefficient is also seen in the energy averaged sticking coefficient (see Fig. 7).

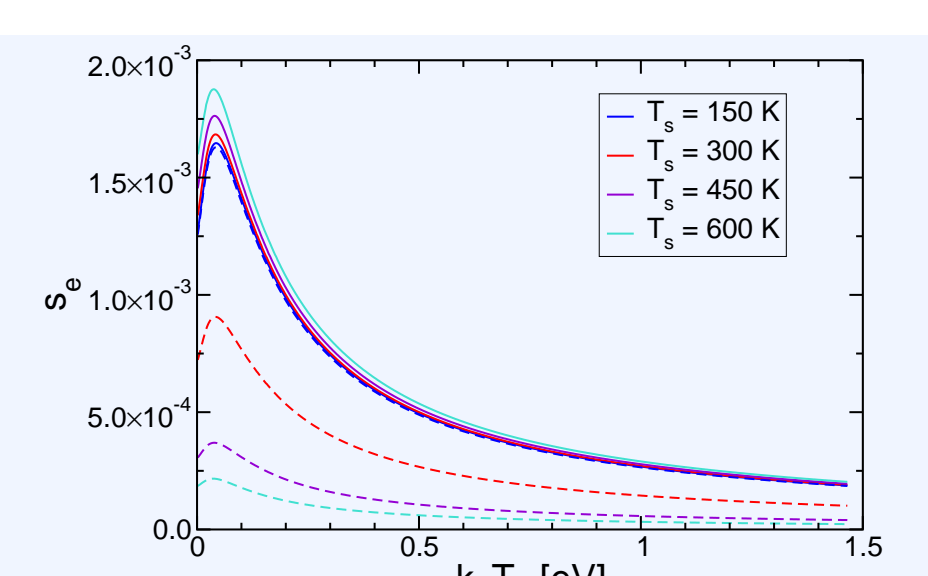


Fig. 7: Prompt (full line) and kinetic (dashed line) energy averaged sticking coefficient for different surface temperatures for a two-phonon deep potential ($T_D = 2500K$).

4 Summary

Employing a simple model for the polarisation-induced interaction between an electron and a dielectric surface, we have investigated desorption and sticking of an electron at a dielectric surface.

Scenarios for desorption and sticking depend both on the surface temperature and the potential depth. Whilst multiphonon processes add very little to the prompt sticking coefficient, they control the relaxation to the lowest bound state so that in some circumstances a trapped electron has only a slim chance of desorbing from the lowest bound state, and is more likely to rejoin the continuum from the upper bound states.

5 References

- [1] F. X. Bronold *et al.*, Eur. Phys. J. D 54, 519 (2009)
- [2] R. L. Heinisch *et al.*, arXiv:1001.4956.